THE HERA CHALLENGES FOR LHC*

Halina Abramowicz

The Raymond and Beverly Sackler School of Physics and Astronomy
Tel Aviv University, 69978 Tel Aviv, Israel

(Received May 16, 2009)

Over the last two decades, the HERA collider has provided a large amount of new information about QCD dynamics at high energy. While the most appreciated are the measurements of the proton structure functions in a wide range of parton momentum x and virtuality Q^2, it is hard to believe that some of the observations at HERA which do not fit the simple picture of DGLAP dynamics would not get amplified at the LHC, possibly rendering certain approaches to searches beyond the Standard Model inadequate.

PACS numbers: 12.38.Aw, 12.38.Bx, 12.39.St, 13.60.–r

1. Introduction

Progress in the next decade (and most probably even longer) in High Energy Physics will be totally overshadowed by the results expected from the Large Hadron Collider (LHC) at CERN (Geneva) where high energy protons will collide at an unprecedented center of mass energy of 14 TeV, any time soon. For quite some time, theorists claim that the success of the Standard Model (SM) of the unified electroweak interactions and of strong interactions cannot be understood, unless it is a low energy realization of a more sophisticated construct, which should manifest itself already at TeV scales. It still remains to be seen whether the Standard Model Higgs, whose mass is constrained by precision electroweak measurements [1], is realized in nature. A low mass of the SM Higgs, about 120 GeV, creates the so-called hierarchy problem, that is the need at high energy for a tremendous fine-tuning of quantum-loop corrections to keep the Higgs mass light enough for it to be relevant for electroweak symmetry breaking. The favored candidates for the new horizon are supersymmetric (SUSY) theories and/or theories

* Presented at the Cracow Epiphany Conference on Hadron Interactions at the Dawn of the LHC, Cracow, Poland, January 5–7, 2009.

with universal extra-dimensions (UED). There are many realizations of these theories (see [2] for a recent overview). Their common denominator is the appearance of new particles or states, which will be signaled by a departure of the measured cross-sections from expectations of the SM.

The generic LHC signatures of SUSY models are isolated leptons, few energetic jets and, for R-parity conserving SUSY, large missing transverse energy [3]. Similar signatures may be expected in the various realizations of the UED theories [4, 5]. These signatures may also originate from the SM, dominated by hard QCD interactions. In the context of LHC physics, QCD constitutes the background (though for many it is in itself a interesting laboratory for the dynamics of high energy QCD). The question is then how reliable is the background estimate. This is where the QCD studies at the HERA ep collider become very relevant, though the energy scales are mostly lower than the ones expected at LHC. The same could be said of the Tevatron $p\bar{p}$ collider studies, if not for the fact that the problems encountered at the Tevatron can only become worse at the LHC. And this is because of the composite nature of hadrons, nucleons in this particular case, which have a rich dynamical internal structure, that cannot be derived from perturbative QCD. This structure is directly probed in the deep inelastic scattering (DIS) of leptons on hadrons.

2. Hard pp interactions

The reactions that will be mostly investigated at the LHC are hard pp interactions in which partons in the proton, quarks and gluons, interact producing either high transverse momentum partons that materialize in the form of hadronic jets or new heavy particles which decay into leptonic and/or hadronic final states. The cross-section for the hard interactions can be calculated in perturbative QCD, though to a limited precision due to higher order corrections. The hadronization process is soft in nature and requires modeling. Due to the complicated nature of resulting final states, even the expectations from pure QCD processes require MC simulation, which limit the precision with which the QCD background can be estimated.

There are the following four components in modeling hadronic final states in hard pp collisions [6]:

1. The hard subprocess at the parton level. At leading order it is a $2 \to 2$ process and the cross-section is expressed through

$$\frac{d\sigma_{\rm int}}{dp_{\rm T}^2} = \sum_{i,j,k} \int dx_1 \int dx_2 \int d\hat{t} f_i\left(x_1, Q^2\right) f_j\left(x_2, Q^2\right) \frac{d\hat{\sigma}_{ij\to kl}}{d\hat{t}} \delta\left(p_{\rm T}^2 - \frac{\hat{t}\hat{u}}{\hat{s}}\right) , \quad (1)$$

where $p_{\rm T}$ is the transverse momentum of the outgoing partons k and l and $\hat{s} = x_1 x_2 s$ is the squared center of mass energy of the partonic

scattering, with s the pp center of mass energy squared and $x_{i,j}$ the fraction of the proton momenta carried by the incoming partons i and j. The cross-section for parton scattering is given by $\hat{\sigma}$, calculable in perturbative QCD, and the probability of finding the partons in the proton is given by the parton density functions (PDF) $f_i(x, Q^2)$, where the hard scale Q^2 is assumed to be $Q^2 = p_{\mathrm{T}}^2$. The variables $\hat{t}$, $\hat{u}$ and $\hat{s}$ are the usual Mandelstam variables.

2. Initial and final state gluon radiation from the interacting partons, which is meant to mimic higher order QCD processes.
3. Additional semi-hard or hard interactions between the remaining partons. They arise naturally in that the integrated cross-section given by (1) diverges for low p_{T} values and σ_{int} becomes bigger than the total cross-section, unless multi-parton interactions (MPI) are introduced.
4. Hadronization, the formation of hadrons from partons and from beam remnants.

Each of these steps is subject to modeling and various Monte Carlo generators [7–11] adopt different approaches, in particular for the last three steps. Each one of the modeling steps is accompanied by uncertainties that are hard to quantify. In the following, the discussion will focus on the extraction of parton density functions which are essential for the calculation of the cross-sections and on the validity of the DGLAP evolution in describing the QCD dynamics at high energy.

3. Parton density functions in the proton

There are many parameterizations of the proton PDFs derived in global fits of the NLO DGLAP evolution equations to the proton structure functions and hard scattering measurements. The most commonly used are the ones provided by the MRST(MSTW) [12] and the CTEQ groups [13]. They incorporate not only the DIS data, but also data from hadron–hadron interactions. A big effort is now vested in quantifying the uncertainties [14] for the precision measurements at the LHC. The worrisome part is that these uncertainties usually come out smaller than the differences between the various groups and this is particularly true with the gluon distribution, the contribution of which dominates the QCD cross-section at LHC.

Recently, the two HERA experiments, H1 and ZEUS, provided the most precise PDFs by combining their HERAI measurements of the F_2 structure function of the proton [15]. The "cross-calibration" reduces dramatically the systematic uncertainties, as shown in Fig. 1. Soon, one may expect even better precision, when the high luminosity measurements of neutral current and charged currents $e^{\pm}p$ interactions from HERAII become available.

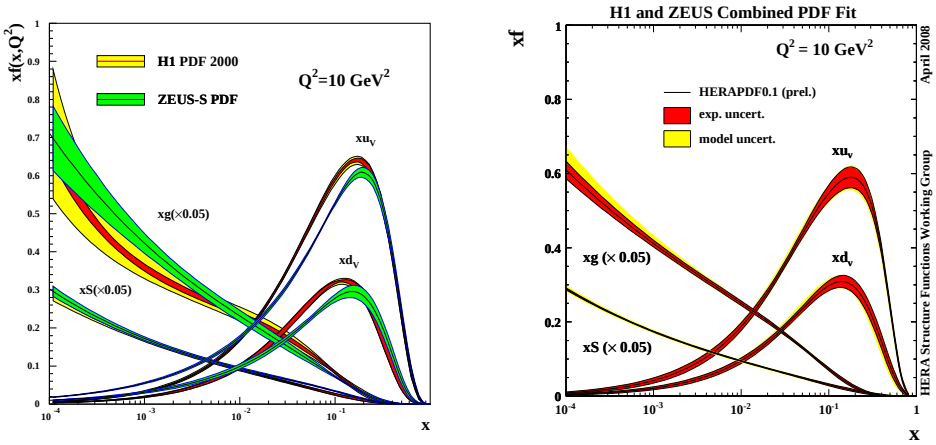

Fig. 1. Left: Comparison of the H1 and the ZEUS PDFs as a function of x at $Q^2 = 10\,\mathrm{GeV}^2$. Right: The result of fitting PDFs to the combined measurements of F_2 at the same Q^2 value.

3.1. Low x regime

The extraction of PDFs assumes the validity of the DGLAP evolution equation in the full range probed by the data, including the very low x regime of HERA. The only marker justifying this approach is the good χ^2 of the global fit. However, many parameters are involved and the lever arm at low x is relatively small (see Fig. 2).

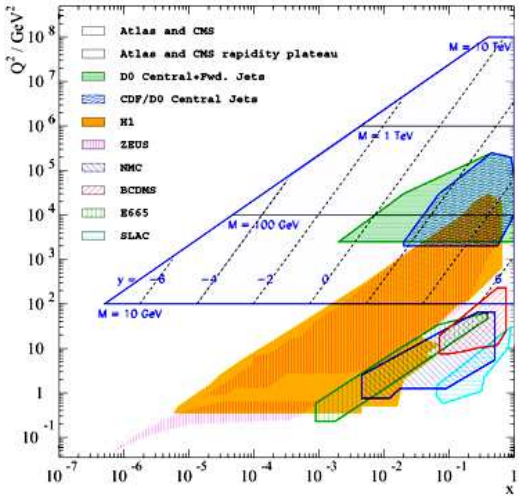

Fig. 2. The coverage of the x and Q^2 plane by existing measurements and the expected coverage in the LHC pp experiments.

A large fraction of the low x cross-section in ep scattering is due to heavy flavor production, in particular $c\bar{c}$ pairs. A compilation of HERA measurements [16] of F_2^{cc}, the contribution of charm production to F_2, is shown in Fig. 3. The treatment of heavy flavor contribution to F_2 is constantly evolving [17] and even within the same scheme there are large differences in the expectations of various groups, which must affect the uncertainty on the gluon distribution.

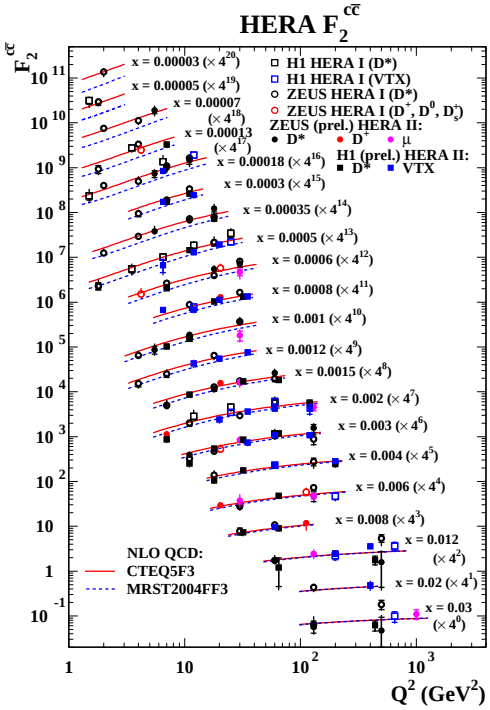

Fig. 3. Compilation of F_2^{cc} as a function of Q^2 for different values of x, compared to expectations of two particular PDFs obtained with the fixed flavor scheme.

In the DGLAP evolution equations, large gluon densities are expected at low x. If the gluon density per unit area becomes large, the probability of recombination of gluons becomes high and non-linear effects in the evolution may show up [18] which would slow down the increase of the gluon density. In addition coherent effects may be expected [19]. It is quite clear by now, that the HERA data do not have the power to rule out or confirm the presence of such effects. However, there are indications in the HERA data that the low x regime of DIS scattering may not be fully described by the DGLAP dynamics. This is exemplified by the large fraction of diffractive-like events as well as by the observation of an excess of forward jets in the low x regime.

4. Diffractive scattering in DIS

If particle production in hard scattering is driven by the DGLAP evolution, large rapidity gaps (LRG) between hadrons are exponentially suppressed. Yet, at HERA, about 10% of the DIS events have a large rapidity gap, which separates the initial proton from the rest of the hadronic final state [20]. It is conceivable that the origin of these LRG is soft in nature and that their presence is accounted for in the initial conditions of the evolution, which would preserve the validity of the DGLAP dynamics in sufficiently hard processes.

The presence of LRG at high energy is associated with diffractive scattering which, in soft hadron–hadron collisions, is believed to be due to the exchange of a Regge trajectory [21] with vacuum quantum numbers — the Pomeron ($I\!P$). The $I\!P$ trajectory is characterized by two parameters, the intercept $\alpha_{I\!P}(0)$ and the slope $\alpha'_{I\!P}$. Both have been determined in soft interactions and the most commonly cited values are $\alpha_{I\!P}(0) = 1.08$ [22] and $\alpha'_{I\!P} = 0.250$ GeV^{-2} [23]. The intercept drives the energy dependence of the total cross-section, $\sigma_{\rm tot} \propto s^{\alpha_{I\!P}(0)-1}$. The value of $\alpha_{I\!P}$ was later updated [24] to $\alpha_{I\!P}(0) = 1.096^{+0.012}_{-0.009}$.

The measurements of the diffractive cross-section in DIS can be used to extract the value of $\alpha_{I\!P}(0)$ [25, 26]. A compilation based on the ZEUS measurements [26] is presented in Fig. 4. The extracted value of $\alpha_{I\!P}(0)$

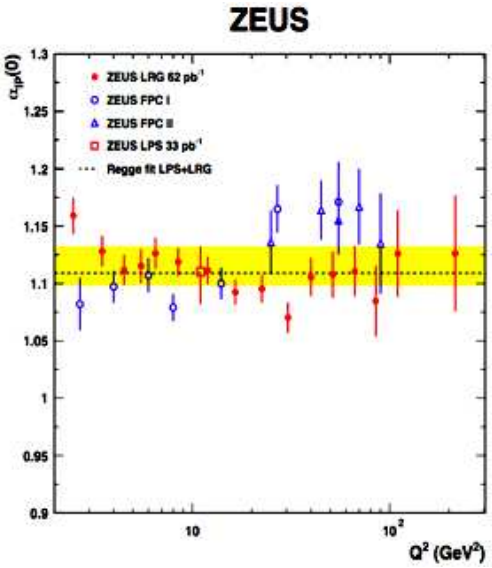

Fig. 4. The value of $\alpha_{I\!P}(0)$ extracted from diffractive DIS scattering as a function of Q^2. The dashed line with the yellow band represents the average value with its uncertainty.

is shown as a function of Q^2 and no dependence on Q^2 is observed. The averaged value of $\alpha_{I\!P}(0)$ in DIS tends to lie above the one derived from soft hadron–hadron interactions. A larger value of $\alpha_{I\!P}(0)$ would imply a faster growth of the cross-section with energy and diffractive scattering in DIS a harder process than in hadron–hadron scattering.

5. QCD factorization in diffraction

The diffractive contribution to the inclusive structure function F_2 is called F_2^{D}. In addition to the usual DIS variables, F_2^{D} also depends on variables which describe the diffractive final state,

$$t = \left(p - p'\right)^2 , \tag{2}$$

$$x_{I\!P} = \frac{q \cdot (p - p')}{q \cdot p} , \tag{3}$$

$$\beta = \frac{Q^2}{2q \cdot (p - p')} = \frac{x}{x_{I\!P}} . \tag{4}$$

Here p and p' respectively denote the proton four-vector before and after the scattering, q is the four-vector of the virtual photon γ^* with $Q^2 = -q^2$. The variable t is the square of the four-momentum exchanged in the proton vertex. The variable $x_{I\!P}$ is the fractional proton momentum which participates in the interaction with γ^* (sometimes denoted by ξ), β is the equivalent of Bjorken x but relative to the exchanged object and $x_{I\!P} \cdot \beta = x$. QCD factorization is expected to hold for F_2^{D} [27–29] and it may then be decomposed into diffractive parton distributions (DPDF), f_i^{D}, in a way similar to the inclusive F_2,

$$\frac{dF_2^{\mathrm{D}}(x, Q^2, x_{I\!P}, t)}{dx_{I\!P} dt} = \sum_i \int_0^{x_{I\!P}} dz \frac{df_i^{\mathrm{D}}(z, \mu, x_{I\!P}, t)}{dx_{I\!P} dt} \hat{F}_{2,i}\left(\frac{x}{z}, Q^2, \mu\right) , \tag{5}$$

where $\hat{F}_{2,i}$ is the universal structure function for DIS on parton i, μ is the factorization scale at which f_i^{D} are probed and z is the fraction of momentum of the proton carried by the diffractive parton i. Diffractive partons are to be understood as those partons in the proton from which the scattering leads to a diffractive final state. The DGLAP evolution equation applies in the same way as for the inclusive case. For a fixed value of $x_{I\!P}$, the evolution in x and Q^2 is equivalent to the evolution in β and Q^2.

If, following Ingelman and Schlein [30], one further assumes the validity of Regge factorization, F_2^{D} may be decomposed into a universal $I\!P$ flux and the structure function of the $I\!P$,

$$\frac{dF_2^{\mathrm{D}}\left(x,Q^2,x_{I\!P},t\right)}{dx_{I\!P}dt} = f_{I\!P/p}(x_{I\!P},t)F_2^{I\!P}\left(\beta,Q^2\right)\ , \tag{6}$$

where the normalization of either of the two components is arbitrary. It implies that the $x_{I\!P}$ and t dependence of the diffractive cross-section is universal, independent of Q^2 and β, and given by

$$f_{I\!P/p}(x_{I\!P},t) \sim \left(\frac{1}{x_{I\!P}}\right)^{2\alpha_{I\!P}(0)-1} e^{\left(b_0^D - 2\alpha'_{I\!P}\ln x_{I\!P}\right)t}\ , \tag{7}$$

one of the expectations which agrees with the measurements as discussed in the previous section.

In this approach, the mechanism for producing LRG is assumed to be present at some scale and the evolution formalism allows to probe the underlying partonic structure. The latter depends on the coupling of quarks and gluons to the Pomeron.

An example of diffractive parton distributions derived by the H1 experiment is shown in Fig. 5 [25]. As in the case of the proton PDF, the gluons are not well constrained by the inclusive measurements. They are further

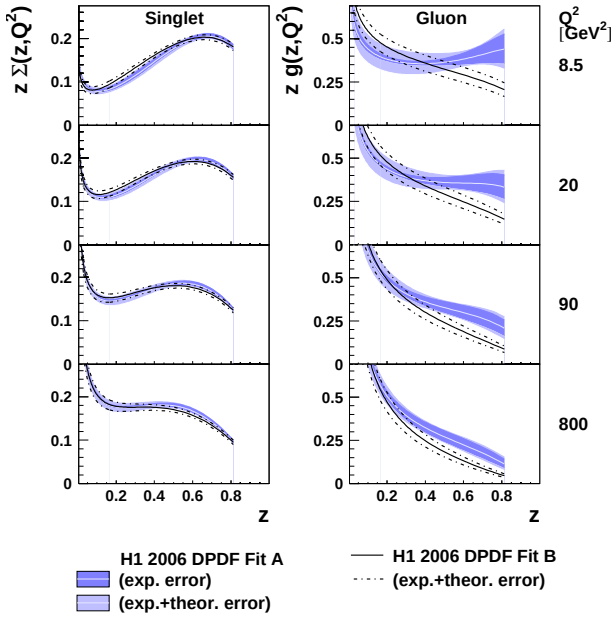

Fig. 5. The singlet, Σ, and the gluon distribution in diffractive parton distributions as a function of the fraction z of the momentum of the colorless exchange responsible for the LRG and for different Q^2 values. Two different fit results are presented as described in the figure.

constrained by diffractive jet [31] and heavy flavor [32, 33] production. The fact that all diffractive DIS data can be accommodated by the same set of DPDF lands support to QCD factorization.

Gluons constitute a large fraction (about 70%) of the diffractive exchange, implying that DIS induced by gluons is more likely to lead to a diffractive final state. In the black-body limit the fraction of diffractive events cannot exceed 50% [34, 35]. At HERA, this limit is far from being reached, however the dominance of gluons in diffractive scattering indicates that the onset of unitarity effects may first show up in the gluon.

6. QCD factorization breaking in diffractive scattering

QCD factorization in diffractive scattering is expected to break down in hadron–hadron interactions [27]. Indeed, the measurements of diffractive dijet production in $p\bar{p}$ interactions at the Tevatron [36] indicate that their rate is by factor 5 to 10 lower than expected from the DPDF extracted at HERA. This is shown in Fig. 6, where the relative rate of diffractively produced dijets is shown as a function of β. The suppression of hard diffrac-

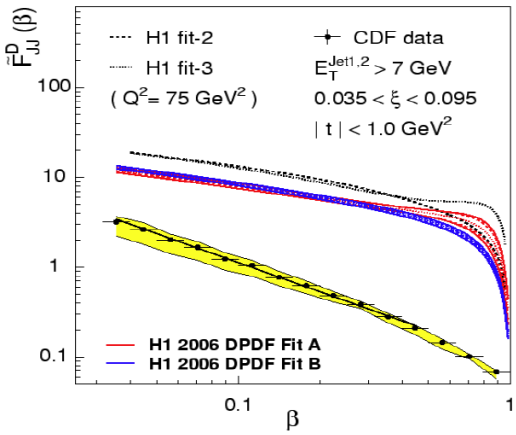

Fig. 6. The ratio of diffractively produced dijets to inclusive dijets as a function of β in $p\bar{p}$ collisions compared to expectations of various DPDFs, as indicated in the figure, extracted from the HERA data.

tive scattering in $p\bar{p}$ is understood as due to rescattering of partons which did not directly participate in the diffractive process. As a result of the rescattering, the LRG is destroyed. This is depicted schematically in Fig. 7. Some suppression of LRG events is also expected in photoproduction (γp) at HERA [37], especially in the regime of resolved photon contributions. In that respect, the data is not conclusive as the H1 experiment observes

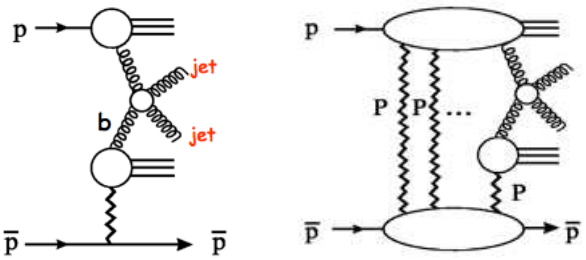

Fig. 7. Left: Diagram for diffractive dijet production in $p\bar{p}$ scattering. Right: Diagram for diffractive dijet production with rescattering.

a large suppression for both the resolved photon (more hadron-like) and the direct photon (more DIS-like) contributions [38] while the ZEUS experiment sees very little suppression if at all [39]. The explanation may lie in the preliminary measurements of the H1 experiment [40] where the cross-section for diffractive dijet production in γp is compared to expectations (assuming QCD factorization) as a function of the highest transverse energy of the two jets, $E_{\mathrm{T}}^{\mathrm{jet}}1$. As shown in Fig. 8, the suppression of LRG events is strongest at low $E_{\mathrm{T}}^{\mathrm{jet}}1$. This is an interesting observation which indicates that the se-

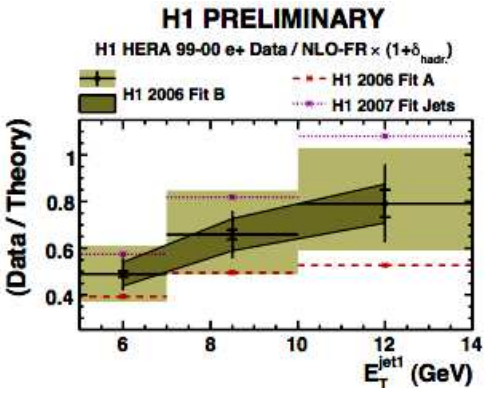

Fig. 8. The ratio of dijet diffractive cross-section to NLO expectations obtained with various DPDFs assuming the validity of QCD factorization as a function of the highest transverse energy of the two jets, $E_{\mathrm{T}}^{\mathrm{jet}}1$.

lection of higher E_{T} jets renders rescattering less probable. In fact, a closer inspection of the CDF results (see Fig. 6) leads to a similar conclusion. The LRG suppression seems stronger at high β, that is lower diffractive masses and therefore lower E_{T} jets. The selection of higher E_{T} jets may be a way of

selecting a (transversely) smaller partonic configuration of the dissociating particle, for which by virtue of color screening the probability of rescattering becomes smaller.

The comparison of the diffractive measurements at HERA and at the Tevatron leads to the following puzzle. Of the order of 10% of events observed in ep collisions cannot be accounted for in $p\bar{p}$ collisions, yet inclusive factorization seems to be preserved (universality of proton PDF). The only explanation is that the mechanism of rescattering somehow preserves the total cross-section. This must have implications for multi-parton interactions, one of the big unknowns at LHC.

7. Hard diffraction and the 3D structure of the proton

A small fraction of diffractive events in ep scattering at HERA consist of exclusive vector meson or single photon (deeply virtual Compton scattering DVCS) production. At the high center of mass energies of HERA and in the presence of a large scale, these exclusive processes are believed to be mediated by two gluon exchange [41, 42]. The cross-section for the exclusive processes is expected to rise with center of mass energy W, with the rate of growth increasing with the value of the hard scale. This is illustrated in Fig. 9 where the W dependence of the γp cross-section for exclusive ρ, ϕ, J/ψ, $\psi(2S)$ and Υ production is shown together with the W dependence of the total γp cross-section (for a detailed discussion and references see [43]). The W dependence of the latter is typical of soft interactions. Also shown

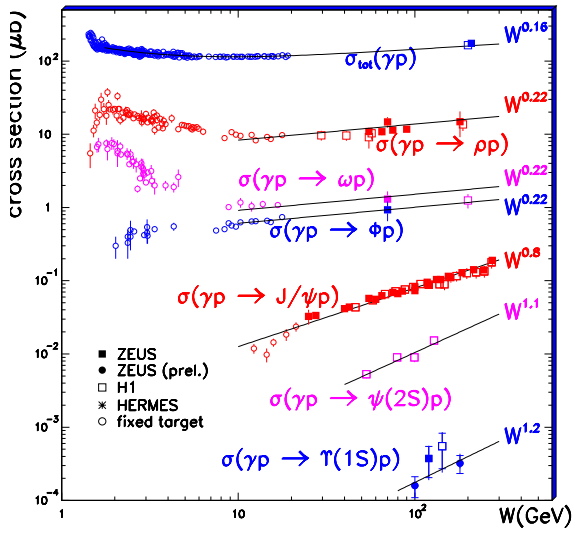

Fig. 9. Total and exclusive vector meson photoproduction cross-sections, as a function od W. The curves are fits of the form $\sim W^{\delta}$.

in the figure are the values of the logarithmic derivative δ obtained by fitting a W^{δ} dependence. Starting from exclusive J/ψ production there is a definite change in the W dependence, with the tendency for δ to become larger as the mass of the vector meson increases. This is interpreted as the evidence of gluon participation in the interaction, since the higher the scale at which the gluons are probed the faster the rise with W.

A further compilation of logarithmic derivatives [43], which also includes the measurements of exclusive processes in DIS, for ρ, ϕ, J/ψ and DVCS as a function of scale defined as $Q^2 + M^2$, where M is the mass of the vector meson, is presented in Fig. 10. With increasing hardness of the interaction, the t distribution is expected to become universal, independent of the scale and of the final state. This is because the harder the scale the more point-like the virtual photon becomes. The exponential slope of the t distribution, b, reflects then the size of the proton. A compilation of measured b values (see [44] for details and references therein) is presented in Fig. 10. Around $Q^2 + M^2$ of about $15\,\mathrm{GeV}^2$ the b values becomes universal.

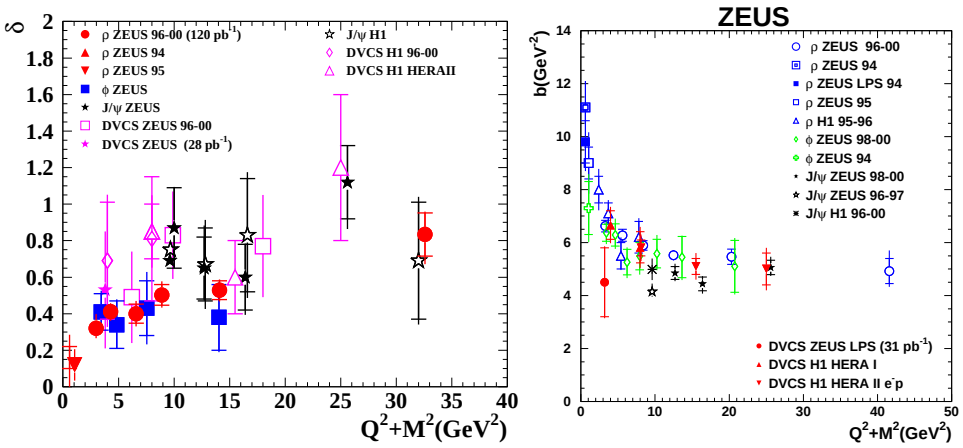

Fig. 10. Left: Logarithmic derivatives $\delta = d\log\sigma(\gamma^* p)/d\log W$ as a function of $Q^2 + M^2$ for exclusive processes. Right: Exponential slope of the t distribution measured for exclusive processes as a function of $Q^2 + M^2$.

Since exclusive vector meson production or DVCS at HERA energies is driven by gluons, the b value probes the size of the gluon cloud in the proton [45]. The universal value of $b \simeq 5\,\mathrm{GeV}^{-2}$ corresponds roughly to a radius of 0.6 fm which is smaller than the 'charge' radius of the proton which is 0.8 fm. This is the first indication that the gluons are well contained within the proton. This finding has implications for multi-parton interactions. In particular the more central the pp interaction the higher the probability of a second partonic interaction [45].

8. Hadronic final states

At LHC, much of the background estimates rely on proper simulations of the hadronic final states, of which multi-parton interactions are only one of the elements.

Most of the MC generators base the formation of the hadronic final state on the properties of the DGLAP dynamics, for which subsequent emissions of partons, before and after the hard interaction, are strongly ordered in transverse momentum k_{T}, with k_{T} increasing steadily while the momentum fraction x decreases. At low x, where effects of the BFKL [46] dynamics may be felt, the ordering in k_{T} may be lost while subsequent emissions are strongly ordered in x. The two different mechanisms are schematically depicted for DIS in Fig. 11. Note that the contribution of large higher order corrections to the DGLAP evolution may also appear as loss of k_{T} ordering. The loss of strong k_{T} ordering may result in the appearance of high E_{T} forward (in the proton direction) jets, of jets with $E_{\mathrm{T}} > Q$ and a decorrelation in the azimuthal angle between jets. All of these effects have been observed at HERA.

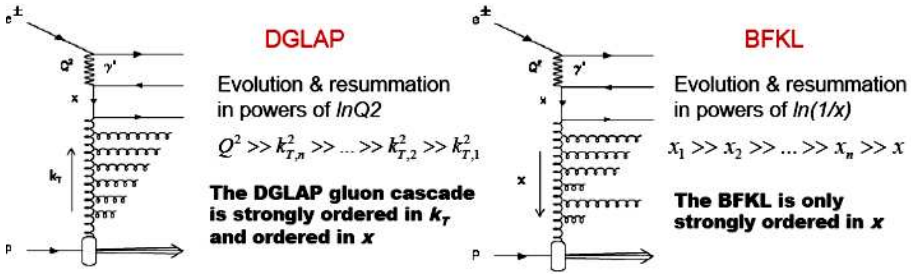

Fig. 11. Schematic representation of the DGLAP (left) and BFKL (right) parton radiation patterns.

The cross-section for producing forward jets, defined by $1.7 < \eta^{\mathrm{jet}} < 2.8$, $x_{\mathrm{jet}} > 0.035$ and with transverse momentum p_{T} fulfilling $0.5 < p_{\mathrm{T}}^2/Q^2 < 5$, as measured by the H1 experiment [47], is shown in Fig. 12 as a function of x.

The measurements are compared to various MC generators. A clear excess of forward jets is observed at low x, which cannot be accounted for neither by higher order DGLAP corrections nor by any other MC generator. The highest rate is expected in the Color Dipole Model (CDM) [48] generator in which the lack of k_{T} ordering is implicit in the way the color dipoles emit radiation. If the DGLAP dynamics, as represented by the RG generator [49], is supplemented by the addition of a resolved virtual photon contribution [50], the rate of forward jet production increases but still fails to describe the lowest x measurements. The addition of a resolved virtual photon contribution is supposed to mimic the lack of k_{T} ordering as shown schematically in Fig. 13.

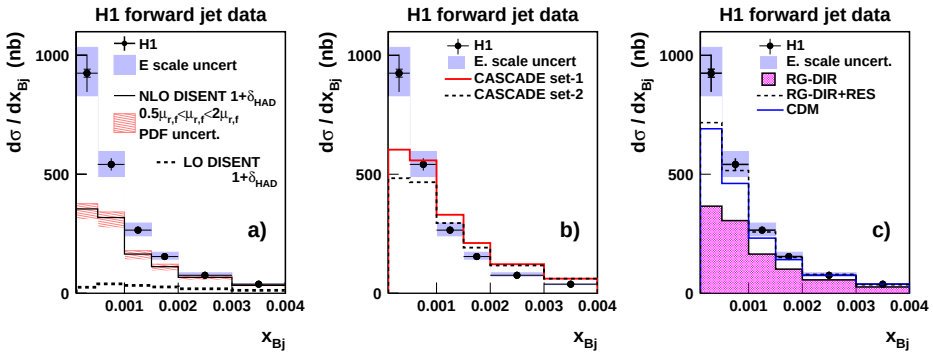

Fig. 12. Cross-section for producing forward jets, with $1.7 < \eta^{\text{jet}} < 2.8$, $x_{\text{jet}} > 0.035$ and with transverse momentum p_{T} fulfilling $0.5 < p_{\text{T}}^2/Q^2 < 5$ as a function of Bjorken x, x_{Bj}. Also shown are expectations of NLO calculations and various MC generators.

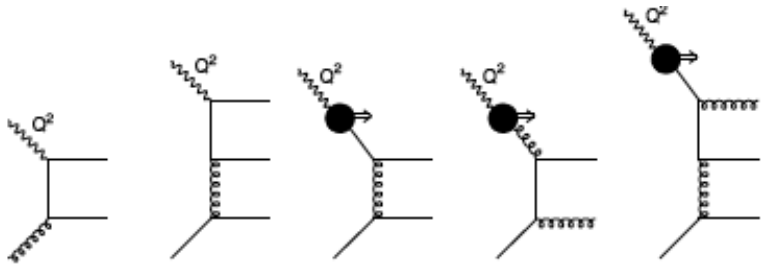

Fig. 13. Schematic representation of diagrams with direct (DIS) and resolved γ^* contributions included in the simulation of DIS hadronic final states.

The addition of a resolved photon contribution also helps in describing the cross-section for dijet production in DIS, in particular in the regime where the E_{T}^2 of the jets is higher than Q^2 [51]. This is shown in Fig. 14 where the dijet differential cross-section is plotted as a function of x_γ^{jets}, the estimator of the γ^* momentum carried by the two jets, for various ranges of transverse energy measured in the $\gamma^* p$ center of mass system, E_{T}^*, and Q^2. However, even the addition of the resolved photon contribution falls short of describing the low Q^2 region where x is lowest.

The azimuthal correlations in multijet production have been measured both by the H1 [52] and the ZEUS [53] experiments. The NLO calculations of dijet production fail to describe the rate of jets with the difference in azimuthal angle $\Delta\phi < 120^\circ$ as shown in Fig. 15, in particular at low x. However, an addition of α^3 terms seems to cure the problem and also properly describes the rates for trijet events.

All these findings strongly suggest that at low x the description of hadronic final states requires corrections even beyond NLO DGLAP.

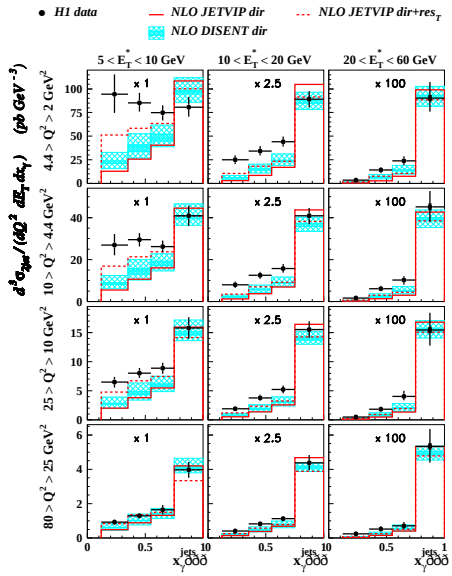

Fig. 14. Cross-section for dijet production as a function of x_γ^{jets}, the estimator of the γ^* momentum carried by the two jets, for various ranges of transverse energy measured in the $\gamma^* p$ center of mass system, E_{T}^*, and Q^2. Also shown are predictions of NLO calculations with and without the resolved γ^* contribution.

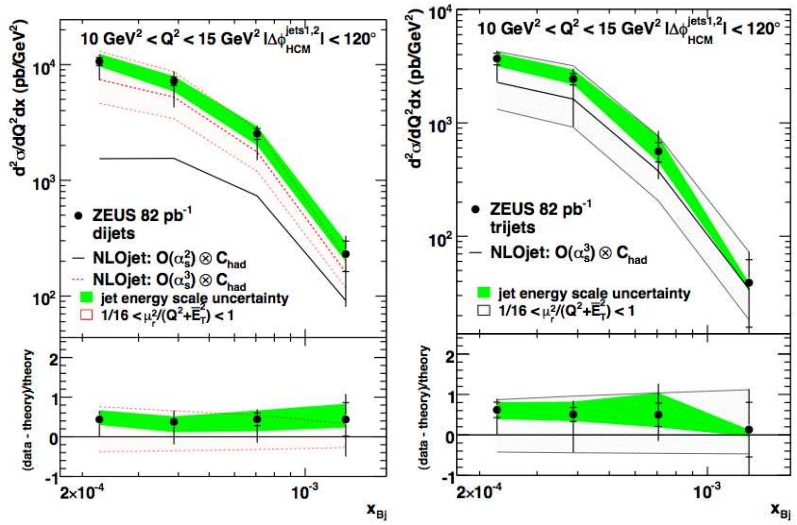

Fig. 15. DIS cross-section for dijet and trijet production, when the two highest E_{T} jets are separated by an azimuthal angle $\Delta\phi < 120°$, as a function of Bjorken x–x_{Bj}. Also shown are the expectations of NLO calculations without and with $\mathcal{O}(\alpha_{\mathrm{s}}^3)$ corrections.

9. Summary

The large fraction of DIS diffractive events, mainly driven by gluons, could suggest the approach to the unitarity limit, in which case non-linear effects could bias the measurements. The observation of an excess of forward jets in the low x regime would suggest that the transverse momentum ordering of gluon radiation, inherent in the DGLAP evolution, breaks down at low x. The same conclusion may be derived from the appearance of the so called 'resolved photon' contribution necessary to described DIS dijet production in the low x regime. At HERA, all these effects constitute a relatively small fraction of the total cross-section (typically 5%) and therefore may not be visible in the fully inclusive measurements. At LHC, these low x effects may be greatly enhanced. In particular, the increased jet multiplicity and the shift of the high transverse momentum activity toward the proton direction could result in events with missing transverse energy greater than expected from Monte Carlo generators.

The non-uniform space distribution of partons in the proton, partly covered by the newest generation of MC programs, and the strong breaking of diffractive QCD factorization due to rescattering, with potentially non-trivial dependence on kinematics, may lead to surprises in modeling the underlying event and multi-parton interactions accompanying hard pp interactions at the LHC.

I would like to thank the organizers of the meeting for inviting me to this stimulating event in memory of Prof. Jan Kwiecinski. I myself belong to the generation of physicists who were inspired by Jan and much of our perseverance at HERA in exploring the QCD dynamics at low x is due to his teachings.

REFERENCES

[1] P. Renton, Global Electroweack Fits the Higgs Boson Mass, Presented at 34th International Conference on High Energy Physics (ICHEP 2008), Philadelphia, Pennsylvania, 2008, arXiv:0809.4566 [hep-ph].

[2] G. Gabadadze, Beyond the Standard Model: Extra Dimensions and Supersymmetry, Prepared for European School on High-Energy Physics, Tsakhkadzor, Armenia, 2003; J. Ellis, *Eur. Phys. J.* **C59**, 335 (2009) [arXiv:0810.1178 [hep-ph]].

[3] P. de Jong, *AIP Conf. Proc.* **1078**, 21 (2009) [arXiv:0809.3708 [hep-ex]].

[4] L. Vacavant, I. Hinchliffe, *J. Phys. G* **27**, 1839 (2001).

[5] A. Datta, K. Kong, K.T. Matchev, *Phys. Rev.* **D72**, 096006 (2005), Erratum *Phys. Rev.* **D72**, 119901 (2005) [arXiv:hep-ph/0509246].

[6] T. Sjostrand, P.Z. Skands, *J. High Energy Phys.* **0403**, 053 (2004) [arXiv:hep-ph/0402078].

[7] T. Sjostrand, S. Mrenna, P. Skands, *J. High Energy Phys.* **0605**, 026 (2006) [arXiv:hep-ph/0603175]; T. Sjostrand, S. Mrenna, P. Skands, *Comput. Phys. Commun.* **178**, 852 (2008) [arXiv:0710.3820 [hep-ph]].

[8] M.H. Seymour, [arXiv:hep-ph/0506202 and references therein; J.M. Butterworth, J.R. Forshaw, M. H. Seymour, *Z. Phys.* **C72**, 637 (1996) [arXiv:hep-ph/9601371]; I. Borozan, M.H. Seymour, *J. High Energy Phys.* **0209**, 015 (2002) [arXiv:hep-ph/0207283].

[9] F.E. Paige *et al.*, arXiv:hep-ph/0312045.

[10] T. Gleisberg *et al.*, *J. High Energy Phys.* **0902**, 007 (2009) [arXiv:0811.4622 [hep-ph]].

[11] M.L. Mangano *et al.*, *J. High Energy Phys.* **0307**, 001 (2003) [arXiv:hep-ph/0206293].

[12] A.D. Martin *et al.*, arXiv:0901.0002 [hep-ph].

[13] P.M. Nadolsky *et al.*, *Phys. Rev.* **D78**, 013004 (2008) [arXiv:0802.0007 [hep-ph]].

[14] The LHAPDF project, see http://projects.hepforge.org/lhapdf/ for details.

[15] B.C. Reisert for the H1 and ZEUS Collaborations, arXiv:0809.4946 [hep-ex].

[16] L. Labarga for the H1 and ZEUS Collaborations, *Nucl. Phys. Proc. Suppl.* **185**, 149 (2008).

[17] R.S. Thorne, R.G. Roberts, *Phys. Lett.* **B421**, 303 (1998) [arXiv:hep-ph/9711223]; C.D. White, R.S. Thorne, *Phys. Rev.* **D74**, 014002 (2006) [arXiv:hep-ph/0603030].

[18] L.V. Gribov, E.M. Levin, M.G. Ryskin, *Phys. Rept.* **100**, 1 (1983).

[19] H. Abramowicz, L. Frankfurt, M. Strikman, *eConf* **C940808**, 033 (1994), *Surveys High Energ. Phys.* **11**, 51 (1997) [arXiv:hep-ph/9503437].

[20] M. Derrick *et al.* [ZEUS Collaboration], *Phys. Lett.* **B315**, 481 (1993); T. Ahmed *et al.* [H1 Collaboration], *Phys. Lett.* **B348**, 681 (1995) [arXiv:hep-ex/9503005].

[21] P.D.B. Collins, *Phys. Rept.* **1**, 103 (1971).

[22] A. Donnachie, P.V. Landshoff, *Phys. Lett.* **B296**, 227 (1992) [hep-ph/9209205].

[23] A. Donnachie, P.V. Landshoff, *Nucl. Phys.* **B231**, 189 (1984).

[24] J.R. Cudell, K. Kang, S.K. Kim, *Phys. Lett.* **B395**, 311 (1997) [arXiv:hep-ph/9601336].

[25] A. Aktas *et al.* [H1 Collaboration], *Eur. Phys. J.* **C48**, 715 (2006) [arXiv:hep-ex/0606004]; *Eur. Phys. J.* **C48**, 749 (2006) [arXiv:hep-ex/0606003].

[26] S. Chekanov *et al.* [ZEUS Collaboration], *Nucl. Phys.* **B816**, 1 (2009) [arXiv:0812.2003 [hep-ex]].

[27] J.C. Collins, *Phys. Rev.* **D57**, 3051 (1998), Erratum *Phys. Rev.* **D61**, 2000 (1998) [hep-ph/9709499].

[28] A. Berera, D.E. Soper, *Phys. Rev.* **D53**, 6162 (1996) [hep-ph/9509239].

[29] L. Trentadue, G. Veneziano, *Phys. Lett.* **B323**, 2001 (1994).

[30] G. Ingelman, P.E. Schlein, *Phys. Lett.* **B152**, 256 (1985).
[31] A. Aktas *et al.* [H1 Collaboration], *J. High Energy Phys.* **0710**, 042 (2007) [arXiv:0708.3217 [hep-ex]].
[32] S. Chekanov *et al.* [ZEUS Collaboration], *Eur. Phys. J.* **C38**, 43 (2004) [arXiv:hep-ex/0408009].
[33] A. Aktas *et al.* [H1 Collaboration], *Eur. Phys. J.* **C50**, 1 (2007) [arXiv:hep-ex/0610076].
[34] J. Pumplin, *Phys. Rev.* **D8**, 2899 (1973).
[35] A.B. Kaidalov, V.A. Khoze, A.D. Martin, M.G. Ryskin, *Phys. Lett.* **B567**, 61 (2003) [hep-ph/0306134].
[36] A.A. Affolder *et al.* [CDF Collaboration], *Phys. Rev. Lett.* **84**, 5043 (2000).
[37] M. Klasen, G. Kramer, *Eur. Phys. J.* **C38**, 93 (2004) [arXiv:hep-ph/0408203].
[38] A. Aktas *et al.* [H1 Collaboration], *J. High Energy Phys.* **0710**, 042 (2007) [arXiv:0708.3217 [hep-ex]].
[39] J. Breitweg *et al.* [ZEUS Collaboration], *Eur. Phys. J.* **C5**, 41 (1998) [arXiv:hep-ex/9804013].
[40] [H1 Collaboration], Diffractive Photoproduction of Dijets in ep Collisions at HERA, H1prelim-08-012, submitted to the XVI International Workshop on Deep Inelastic Scattering, DIS 2008, London.
[41] M.G. Ryskin, *Z. Phys.* **C57**, 89 (1993).
[42] S.J. Brodsky, L. Frankfurt, J.F. Gunion, A.H. Mueller, M. Strikman, *Phys. Rev.* **D50**, 3134 (1994) [arXiv:hep-ph/9402283].
[43] A. Levy, *Acta Phys. Pol. B* **40**, 1775 (2009), these proceedings.
[44] S. Chekanov *et al.* [ZEUS Collaboration], arXiv:0812.2517 [hep-ex].
[45] L. Frankfurt, M. Strikman, C. Weiss, *Ann. Rev. Nucl. Part. Sci.* **55**, 403 (2005) [arXiv:hep-ph/0507286].
[46] L.N. Lipatov, *Sov. J. Nucl. Phys.* **23**, 338 (1976); E.A. Kuraev, L.N. Lipatov, V.S. Fadin, *Sov. Phys. JETP* **45**, 199 (1977); I.I. Balitsky, L.N. Lipatov, *Sov. J. Nucl. Phys.* **28**, 822 (1978).
[47] A. Aktas *et al.* [H1 Collaboration], *Eur. Phys. J.* **C46**, 27 (2006) [arXiv:hep-ex/0508055].
[48] B. Andersson, G. Gustafson, L. Lonnblad, U. Pettersson, *Z. Phys.* **C43**, 625 (1989); L. Lonnblad, *Comput. Phys. Commun.* **71**, 15 (1992); *Z. Phys.* **C65**, 285 (1995).
[49] H. Jung, *Comput. Phys. Commun.* **86**, 147 (1995).
[50] H. Jung, L. Jonsson, H. Kuster, arXiv:hep-ph/9811368; *Eur. Phys. J.* **C9**, 383 (1999) [arXiv:hep-ph/9903306].
[51] A. Aktas *et al.* [H1 Collaboration], *Eur. Phys. J.* **C37**, 141 (2004) [arXiv:hep-ex/0401010].
[52] A. Aktas *et al.* [H1 Collaboration], *Eur. Phys. J.* **C33**, 477 (2004) [arXiv:hep-ex/0310019]; F.D. Aaron *et al.* [H1 Collaboration], *Eur. Phys. J.* **C54**, 389 (2008) [arXiv:0711.2606 [hep-ex]].
[53] S. Chekanov *et al.* [ZEUS Collaboration], *Nucl. Phys.* **B786**, 152 (2007) [arXiv:0705.1931 [hep-ex]].